

Robust Watermarking Using Inverse Gradient Attention

Honglei Zhang* † Hu Wang* ‡ Yidong Li † Yuanzhouhan Cao † Chunhua Shen ‡
 Beijing Jiaotong University, Beijing †
 The University of Adelaide, Australia ‡

Abstract

Watermarking is the procedure of encoding desired information into an image to resist potential noises while ensuring the embedded image has little perceptual perturbations from the original image. Recently, with the tremendous successes gained by deep neural networks in various fields, digital watermarking has attracted increasing number of attentions. The neglect of considering the pixel importance within the cover image of deep neural models will inevitably affect the model robustness for information hiding. Targeting at the problem, in this paper, we propose a novel deep watermarking scheme with Inverse Gradient Attention (IGA), combining the ideas of adversarial learning and attention mechanism to endow different importance to different pixels. With the proposed method, the model is able to spotlight pixels with more robustness for embedding data. Besides, from an orthogonal point of view, in order to increase the model embedding capacity, we propose a complementary message coding module. Empirically, extensive experiments show that the proposed model outperforms the state-of-the-art methods on two prevalent datasets under multiple settings.

1. Introduction

The goal of watermarking is to embed as much as general information into a cover image for the purpose of copyright protection without introducing too much perceptual difference from the cover image. And the embedded message can be robustly reconstructed under image distortions. Hence there are three key factors to measure a watermarking model, *capacity*, *imperceptibility* and *robustness*. The capacity refers to the amount of information that a watermarking model can embed into a cover image, while the imperceptibility refers to the similarity between the cover image and the encoded image. The imperceptibility is a trade-off factor of capacity, as more embedded information leads to larger perceptual differences. The robustness refers

to the reliability of message reconstruction.

The general message embedded by a robust watermarking model can survive under a variety of distortions such as cropping, blurring, or JPEG compression. To achieve this goal, some traditional methods hide messages in texture rich areas [5] or frequent domain [9]. In recent years, some deep learning based methods have achieved outstanding performance. Zhu et al. [19] applied the nature of generative adversarial network (GAN) and learn to use invisible perturbations to encode a rich amount of useful information. Similarly, Luo et al. [12] used GAN as an attack network to generate agnostic image distortions. The watermarking model is more robust than the models trained with known distortions.

Since in a cover image, different pixels have different sensitiveness to noise, some works explore the attention based methods for watermarking. Most recently, Yu et al. [17] proposed to learn an attention mask through a CNN model. The learned attention mask locates the inconspicuous areas of cover images, which are suitable for embedding messages. Nevertheless, they do not take the robustness of each pixel to protect encoded information from distortions into account, which inevitably limits the capability of models to encode more complicated information. In this work, we propose to learn a novel attention mask, known as the Inverse Gradient Attention (IGA). Instead of introducing more parameters, our IGA scheme is non-parametric and the attention mask is generated by calculating the gradients toward message reconstruction loss over the cover image pixels. Additionally, compared with general attention-based models, our model is more explainable because it is gradient-based [7]. The visualization results of our generated attention mask are presented in Fig. 1. The inverse gradient values locate the pixels that are robust for message embedding. Though this simple yet effective method, the proposed IGA model improves the robustness of the watermarking model against various image distortions.

Following the aforementioned GAN based methods, we also apply the generative adversarial learning scheme by introducing a discriminator to predict whether an image contains an encoded image. Hence the imperceptibility of our

*Equal contribution.



Figure 1. Visualization of the some cover images from COCO dataset and their corresponding inverse gradient attention masks generated by our model. **Top:** The cover images. **Bottom:** The inverse gradient attention masks visualized by transferring them into RGB channels. The higher value of each pixel within the attention mask, more attention will be allocated to the corresponding cover image pixels.

model is improved. In addition, in order to improve the capacity of our model, we introduce a message coding module that maps the message onto a low dimensional space before encoding and maps them back to their original space after decoding.

In summary, our main contributions are listed below:

- We apply the idea of adversarial learning to generate inverse gradient attention to perceive more robust pixels in the cover image for data hiding. By doing so, the watermarking is more robust to resist a variety of image distortions.
- We propose a message coding module, as known as Message Encoder and Message Decoder in the framework, to map messages with long length into compressed ones, with the purpose of improving model data hiding capacity.
- We conduct the experiments on two prevalent datasets and instantiate them on multiple state-of-the-art watermarking models. Empirically, our proposed model is able to surpass its counterparts by a large margin and achieve state-of-the-art performance. Moreover, we further identify and discuss the connections between the proposed inverse gradient attention with high-frequency regions within images.

2. Related Work

Follow the development vein of digital watermarking technology, we divide it into two categories for clear explanation: traditional watermarking approaches and deep learning based watermarking approaches.

2.1. Traditional Watermarking Approaches.

The traditional watermarking methods mainly adopt human heuristics and hand-designed methods to select pixels for information embedding. According to the forms and the domains of manipulating pixels, it can be further divided

into spatial domain watermarking [3, 4, 15] and frequency domain watermarking [6, 11, 14]. For the spatial domain watermarking, Tomas et al. [15] proposed the HUGO algorithm to manipulate the least significant bits of certain pixels of the cover image. Banitalebi et al. [4] proposed a robust least significant bit based watermarking model to compute the structural similarity in the process of embedding and extracting watermarks. From the frequency domain perspective, some algorithms changed middle frequency components of the cover image in the frequency domain [6], and others exploited the correlation between discrete cosine transform coefficients of the adjacent blocks [14].

2.2. Deep Learning based Watermarking Approaches.

Due to the strong representation ability of deep neural networks, an increasing number of powerful deep watermarking models have been proposed. [13] adopts convolutional neural networks as a feature extractor of the watermark framework. Recently, the encoder-decoder framework has received more attention for watermarking since it fits the symmetrical encoding and decoding process of information embedding and extraction [2, 12, 17, 19]. Zhu et al. [19] introduced an encoder-decoder framework named HiDDeN, which is a unified end-to-end framework for robust watermarking and steganography. Besides, Luo et al. [12] proposed Distortion-Agnostic model to adversarially add noises by an attacking network to achieve the purpose of adaptive data augmentation and improve the robustness of the watermarking model.

Compared with the existing models, one main difference of our model is that we embrace the idea of adversarial mechanism to generate an inverse gradient attention mask to effectively find robust pixels in the cover image in an end-to-end framework, instead of adding adversarial examples into the training set as data augmentation. In this case, with the proposed method, pixel-level robust regions are spotlighted for watermarking to achieve the purpose of efficient

and adaptive information embedding. Moreover, compared with general attention methods, our model is more explainable due to it is gradient-based [7].

3. Proposed Method

3.1. Overall Architecture

We illustrate the overall architecture of our proposed watermarking method in Fig. 2. It consists of 4 modules: a message coding module, an inverse gradient attention module, an encoder and a decoder. The message coding module consists of a message encoder and a message decoder. The message encoder takes a binary message $\mathbf{M} \in \{0, 1\}^K$ of length K as input and outputs an encoded message $\mathbf{M}_{en} \in \mathbb{R}^D$ of length D , where $D < K$. Then at the end of our architecture, the message decoder is inputted $\mathbf{M}_{de} \in \mathbb{R}^D$ and outputs the recovered message $\mathbf{M}_{out} \in \{0, 1\}^K$ of length K . Given the input message \mathbf{M} and the output message \mathbf{M}_{out} , we can calculate a message reconstruction loss. The inverse gradient attention module generates an attention mask \mathbf{A} , which indicates the gradients of input cover image \mathbf{I}_{co} toward the message reconstruction loss. Intuitively, the gradient values generally show the robustness of each pixel for message reconstruction.

After the attended image \mathbf{I}_{co}^A is fetched from cover image \mathbf{I}_{co} and the attention mask \mathbf{A} , the encoder takes the attended image \mathbf{I}_{co}^A and the encoded message \mathbf{M}_{en} as input and outputs an encoded image \mathbf{I}_{en} . The encoder consists of an image feature extractor and a watermarking network: the feature extractor takes \mathbf{I}_{co}^A as input and outputs image feature map \mathbf{F}_{co} ; the watermarking network takes the encoded message \mathbf{M}_{en} and the attended image feature map \mathbf{F}_{co} as input, and outputs the encoded image \mathbf{I}_{en} . The encoded image is then fed into the decoder to reconstruct the message \mathbf{M}_{de} . Finally the messages decoder takes as input \mathbf{M}_{de} and outputs $\mathbf{M}_{out} \in \{0, 1\}^K$ of length K .

3.2. Message Coding Module

As mentioned above, the capacity of a watermarking model refers to the amount of embedded information. The amount of information embedded in cover images is measured by bits-per-pixel (BPP). The larger the message volume, the higher the BPP value. The amount of information is normally set to 0.4 BPP or lower [16] to maintain a reasonable imperceptibility. In order to enhance the capacity while maintaining the imperceptibility of our proposed watermarking model, we introduce a message coding module. Specifically, we adopt a symmetric encoder-decoder structure for message coding. They are all made up of multi-layer perceptrons with one hidden layer. The message encoder maps the original message onto a low dimensional space for less reconstruction disturbance; the message decoder recovers the dimension of the decoded message to

the original length. Note that our message coding module is different from the channel coding proposed in [12]. The channel coding is to produce a redundant message to enhance the model robustness, while our message coding module is to reduce the dimension of the message to enhance the model capacity. In our watermarking model, we apply the inverse gradient attention (IGA) to enhance the robustness, which we will introduce in the next sub-section.

3.3. Inverse Gradient Attention

For a watermarking model, the embedded message needs to be robustly reconstructed under image distortions. In order to achieve promising robustness, we need to locate the pixels that are robust enough for message reconstruction in the cover image, and then impose the message on these pixels. As described in [7], applying small but intentionally worst-case perturbations towards vulnerable pixels to the original image can result in the model outputting a totally incorrect result with high confidence. Inspired by this work, we propose a simple yet effective way to locate those pixels that are robust for message reconstruction. Specifically, we first calculate a message reconstruction loss $L_{MR}(\mathbf{M}, \mathbf{M}_{out})$ based on the message \mathbf{M} to be encoded and the reconstructed message \mathbf{M}_{out} . Then, an attention mask \mathbf{A} is generated by calculating the inverse normalized gradients of cover image \mathbf{I}_{co} toward the message reconstruction loss L_{MR} through back-propagation. Formally, this process can be presented as:

$$\mathbf{A} = \mathbf{T} - g(\nabla_{I_{co}} L_{MR}(\mathbf{M}, \mathbf{M}_{out})), \quad (1)$$

where \mathbf{T} represents the tensor contains all ones. g denotes the general normalization function which is adopted to constrain the gradient values range from 0 to 1, e.g., sigmoid function or min-max normalization function. It is notable here that the shape of I_{co}^A is the same as the cover image I_{co} .

Intuitively, the inverse gradient attention mask highlights the pixels that are robust for message reconstruction. In this case, we are able to encode messages robustly on these pixels. Particularly, we first obtain the Hadamard product of the cover image \mathbf{I}_{co} with the obtained attention mask \mathbf{A} . The multiplication is performed in a pixel-wise manner, the attended image \mathbf{I}_{co}^A is therefore obtained. Then, the attended image is fed into the feature extractor and the output is concatenated with the encoded message \mathbf{M}_{en} to formulate the input of watermarking network \mathbf{F}_{co}^M :

$$\mathbf{F}_{co}^M = \mathcal{E}(\mathbf{A} \odot \mathbf{I}_{co}) \oplus \mathbf{M}_{en}, \quad (2)$$

where \mathcal{E} is the feature extractor. \mathbf{M}_{en} is generated by the message encoder in the message coding module. \odot denotes the Hadamard product and \oplus represents the concatenation operation.

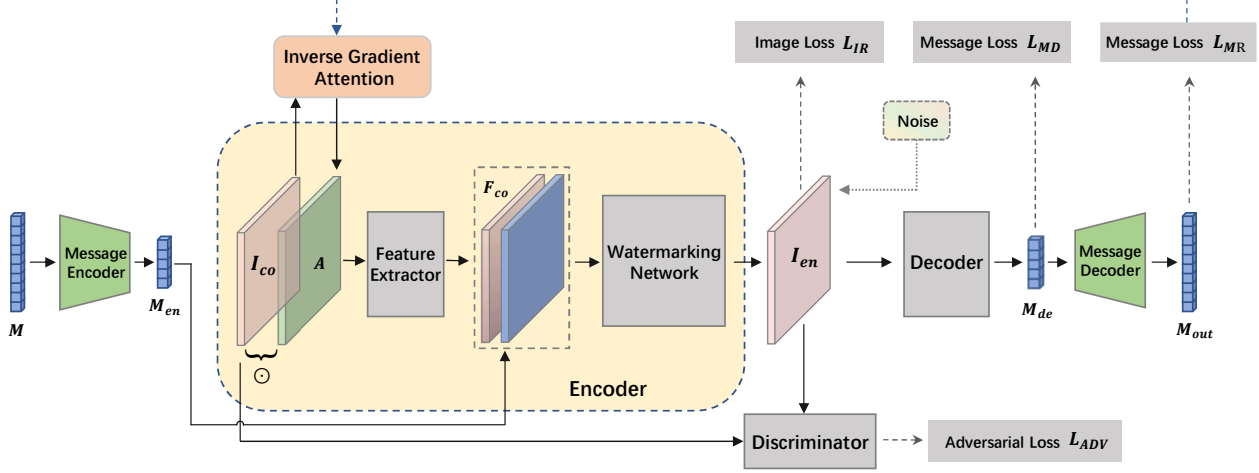


Figure 2. The framework of the proposed IGA model. The message to be embedded \mathbf{M} is fed into the Message Encoder Network to produce a compact encoded message representation \mathbf{M}_{en} . Meanwhile, the inverse gradient attention \mathbf{A} for the cover image \mathbf{I}_{co} is computed for the gradients towards the message reconstruction loss through back-propagation. Once the inverse gradient attention mask \mathbf{A} is fetched, the Hadamard product of it and the cover image \mathbf{I}_{co} is required to obtain the attended image. The intuition behind it is the lower gradient value of a pixel towards the message reconstruction loss, the smaller impact of it to recover the message. Therefore, more weights could be allocated to this pixel and more information can be expected to embed into it. Then, the attended image is fed into the feature extractor \mathcal{E} to produce intermediate feature maps \mathbf{F}_{co} . Later on, the \mathbf{F}_{co} and the encoded message \mathbf{M}_{en} are concatenated to generate the encoded image \mathbf{I}_{en} through the Watermarking Network. Then, the Decoder Network produces a reconstructed decoded message \mathbf{M}_{de} . At last, the decoded message \mathbf{M}_{de} is further fed into the Message Decoder Network to produce the final recovered message \mathbf{M}_{out} . The training process of the framework is optimized under the supervision of the following four losses: Image Reconstruction Loss L_{IR} , Message Decoding Loss L_{MD} and Message Reconstruction Loss L_{MR} , and Generative Adversarial Loss L_{ADV} .

3.4. Loss Functions

We apply four loss functions to train our watermarking model: two message loss functions to ensure the model robustness, an image reconstruction loss and an adversarial loss function to ensure the model imperceptibility. The MSE loss are adopted for two message loss functions that are defined as:

$$L_{MR} = \frac{1}{K} \sum_p (\mathbf{M}(p) - \mathbf{M}_{out}(p))^2, \quad (3)$$

and

$$L_{MD} = \frac{1}{D} \sum_p (\mathbf{M}_{en}(p) - \mathbf{M}_{de}(p))^2. \quad (4)$$

where $\mathbf{M} \in \{0,1\}^K$ and $\mathbf{M}_{out} \in \{0,1\}^K$ represent the input message and the expanded message respectively. $\mathbf{M}_{en} \in \mathbb{R}^D$ and $\mathbf{M}_{de} \in \mathbb{R}^D$ represent the encoded message and the decoded message respectively, and p denotes an element in message. L_{MR} enforces the reconstructed message to be close to the original input, and L_{MD} enforces the decoded message to be close to the encoded message.

We also adopt MSE loss as our image reconstruction loss to enforce the encoded image to be close to the input cover

image:

$$L_{IR} = \frac{1}{N} \sum_{i,j} (\mathbf{I}_{co}(i,j) - \mathbf{I}_{en}(i,j))^2, \quad (5)$$

where \mathbf{I}_{co} and \mathbf{I}_{en} represents the cover and encoded images respectively. i and j represent the pixel location and N is the total number of pixels.

Our model is able to encode a message into a cover image and robustly decoded thanks to the aforementioned objective functions. In order to further enforce the imperceptibility of our model, we adopt a generative adversarial training scheme. Specifically, we treat the encoder as a generator and introduce a discriminator to distinguish if an image is encoded. The objective of our generative adversarial learning is represented as:

$$\min_G \max_D L_{ADV}(G, D) = \mathbb{E}_{\mathbf{x} \in \zeta} [\log(D(\mathbf{x}))] + \mathbb{E}_{\mathbf{x} \in \zeta} [\log(1 - D(G(\mathbf{x})))], \quad (6)$$

where \mathbf{x} is the input cover image and ζ represents its the distributions. Note that the setting of our generative adversarial learning is different from [12]. An image generator in [12] is used to adaptively generate image distortions for the sake of resisting unknown noises. In our work, we evaluate the performance of models on specific distortions such

as cropping, resizing to the encoded image as illustrated in Fig. 2.

4. Experiments

In this section, we first introduce our experimental settings in detail, and then present the extensive experimental results that validate the effectiveness of our model. The experiments contain four parts: in the first two parts, we will compare our approach with other three state-of-the-art digital watermarking methods in three aspects, i.e., *robustness*, *imperceptibility* and *capacity*; the ablation study is further presented to verify the contributions of each component within our framework. Finally, we discuss the relationship between the proposed inverse gradient attention and high-frequency image regions to offer more insights.

4.1. Experimental Settings

Datasets. In order to verify the effectiveness of our proposed model, we utilize two real-world datasets for model training and evaluation, namely the COCO dataset [10] and the DIV2K dataset [1]. For the COCO dataset, 10,000 images are collected for training, and evaluation is performed on the other 1000 unseen images. For the DIV2K dataset, we use 800 images for training and 100 images for evaluation. For each image in the two datasets, there is a corresponding string which is uniformly and randomly sampled with a fixed length.

Evaluation Metrics. To thoroughly evaluate the performance of our model and other watermarking models, we apply a series of evaluation metrics. For model robustness, the bit prediction accuracy is utilized to evaluate the ability of watermarking model to withstand image distortions. It is defined as the ratio of the correct prediction between the input message M_{in} and the corresponding position of the reconstructed message M_{out} . For imperceptibility, we adopt the peak signal-to-noise ratio (PSNR) for evaluation. In addition, we also visually evaluate the encoded images with embedded information. For the model capacity, we apply the Reed-Solomon bits-per-pixel (RS-BPP) [18] as the metric which represents the average number of bits that can be reliably transmitted in an image (the higher the value, the greater the capacity of the embedded information that the algorithm can carry). It is worth noting that these metrics are trade-off to each other. The model with higher capacity often incurs lower imperceptibility. For watermarking tasks, we pay more attention to the model robustness to survive from distortions, under the premise of ensuring imperceptibility and capacity.

Compared Models. To evaluate the effectiveness of our proposed framework in multiple paradigms, we compare a variety of canonical watermarking models. A brief introduction to these methods are listed below:

- HiDDeN [19] is a unified end-to-end CNN model for digital watermarking and image steganography.
- SteganoGAN [18] introduces residual learning into the watermarking process to boost the model performance. It can embed messages with different channel depths as well.
- Distortion-Agnostic [12] can resist unknown image distortions by adaptively adding noises through adversarial learning.

Implementation Details. In our implementation, images are resized to 128×128 for the HiDDeN and the Distortion-Agnostic models, while for the SteganoGAN model, images are resized to 400×400 . We utilize combined noises to train all watermarking models. Specifically, these distortions include *Crop*, *Cropout*, *Resize*, *Dropout* and *Jpeg* compression.

We note here that the parameters of the compared models completely experiment with the settings of the papers for fair comparison. In the training phase, the Adam optimizer [8] with default hyperparameters is adopted. The batch size is set to 32. For the proposed IGA model, the Message Encoder Network and Message Decoder Network are made up of fully connected network with one hidden layer. The Feature Extractor Network, Watermarking Network, Decoder Network and Discriminator Network are all composed of multiple convolution layers.

4.2. Quantitative Analysis on Robustness

In this section, we evaluate the model robustness through the bit prediction accuracy and compare with other watermarking methods. We conduct the experiments on the COCO and the DIV2K datasets. Since in both the HiDDeN model and the Distortion-Agnostic model, the embedded message is one-dimensional binary string $M \in \{0, 1\}^K$, we compare our method with these two methods and illustrate the results in Table 1. As for the SteganoGAN model, the embedded message is a binary tensor $M \in \{0, 1\}^{d \times H \times W}$, we compare our method with the SteganoGAN model and illustrate the results in Table 2.

Table 1 gives a comprehensive comparison with the HiDDeN and the Distortion-Agnostic models across a variety of message lengths and image distortions. We can see from the results that our method outperforms the two methods in the majority of settings. The proposed IGA model surpasses HiDDeN model by 14.52% on COCO dataset and 7.16% on DIV2K dataset under no noise and message length 64 settings. When the message length is 30 or 64, only under a few image distortions that our results are slightly lower. And when the message length is 90, our results are significantly better under all image distortions. Our model surpasses HiDDeN model by 6.91% under Identity setting and

| Methods | COCO | | | | | | | | | DIV2K | | | | | | | | |
|------------|----------|-----------------|--------------|----------------|----------------|---------------|--------------|--------------|-----------------|--------------|----------------|----------------|---------------|--------------|--------------|--|--|--|
| | <i>K</i> | <i>Identity</i> | <i>Crop</i> | <i>Cropout</i> | <i>Dropout</i> | <i>Resize</i> | <i>Jpeg</i> | <i>CN</i> | <i>Identity</i> | <i>Crop</i> | <i>Cropout</i> | <i>Dropout</i> | <i>Resize</i> | <i>Jpeg</i> | <i>CN</i> | | | |
| HiD | 30 | 98.10 | 80.34 | 75.96 | 76.89 | 82.72 | 84.09 | 76.30 | 73.72 | 68.24 | 60.92 | 63.78 | 66.28 | 66.37 | 58.05 | | | |
| | 64 | 79.82 | 72.52 | 63.20 | 68.53 | 69.35 | 68.85 | 65.46 | 70.45 | 50.60 | 51.09 | 49.40 | 50.81 | 49.99 | 49.35 | | | |
| | 90 | 77.56 | 65.46 | 60.20 | 61.49 | 63.03 | 63.21 | 62.07 | 71.04 | 49.63 | 51.50 | 49.22 | 51.40 | 51.16 | 49.84 | | | |
| DA | 30 | 99.50 | 81.15 | 78.58 | 77.13 | 81.72 | 82.83 | 75.73 | 78.80 | 77.32 | 77.11 | 74.55 | 71.01 | 82.35 | 63.85 | | | |
| | 64 | 77.18 | 68.68 | 65.82 | 73.00 | 62.54 | 73.58 | 64.90 | 62.01 | 62.65 | 61.79 | 71.09 | 58.91 | 71.26 | 53.31 | | | |
| | 90 | 70.82 | 63.51 | 61.08 | 64.28 | 62.62 | 67.00 | 63.21 | 57.88 | 58.12 | 54.18 | 57.32 | 55.68 | 62.17 | 53.05 | | | |
| IGA (Ours) | 30 | 99.96 | 86.88 | 79.33 | 77.51 | 81.44 | 87.35 | 80.30 | 79.94 | 77.39 | 60.93 | 76.63 | 72.19 | 82.90 | 64.14 | | | |
| | 64 | 94.34 | 73.34 | 66.82 | 70.23 | 69.41 | 72.07 | 68.38 | 77.61 | 63.11 | 62.00 | 70.14 | 59.64 | 72.31 | 57.03 | | | |
| | 90 | 84.47 | 69.45 | 62.52 | 64.96 | 65.78 | 68.78 | 65.88 | 71.47 | 59.10 | 55.31 | 60.10 | 56.48 | 63.21 | 55.59 | | | |

Table 1. Comparison results with the HiDDeN model (HiD) and the Distortion-Agnostic model (DA) on the COCO and the DIV2K datasets. All models are trained and evaluated with various message lengths and image distortions. We adopt 3 message lengths $K = 30, 64, 90$, and 6 image distortions. *Identity* refers to no distortion and *CN* refers to the random selection of *Crop*, *Cropout*, *Dropout*, *Resize* and *Jpeg* compression during training and evaluation.

| Methods | COCO | | | | DIV2K | | | |
|-------------|----------|-----------------|--------------|-----------------|--------------|--|--|--|
| | <i>d</i> | <i>Identity</i> | <i>CN</i> | <i>Identity</i> | <i>CN</i> | | | |
| SG | 1 | 97.91 | 62.38 | 98.29 | 61.38 | | | |
| | 2 | 96.02 | 62.63 | 96.53 | 58.11 | | | |
| | 3 | 86.19 | 56.64 | 89.10 | 55.86 | | | |
| | 4 | 76.10 | 53.39 | 78.07 | 53.03 | | | |
| | 5 | 70.98 | 53.41 | 71.31 | 52.65 | | | |
| IGA* (Ours) | 1 | 99.67 | 68.70 | 99.39 | 67.65 | | | |
| | 2 | 99.07 | 65.04 | 98.62 | 58.65 | | | |
| | 3 | 95.26 | 59.05 | 95.64 | 57.92 | | | |
| | 4 | 84.56 | 55.78 | 84.28 | 57.46 | | | |
| | 5 | 77.78 | 55.02 | 77.97 | 56.59 | | | |

Table 2. Comparison results with the SteganoGAN model on the COCO and the DIV2K datasets. All models are trained and evaluated with various message lengths and image distortions. We adopt 5 message channels $d = 1, 2, 3, 4, 5$, and 1 image distortion. *Identity* refers to no distortion and *CN* refers to the random selection of *Crop*, *Cropout*, *Dropout*, *Resize* and *Jpeg* compression during training and evaluation. In the table, the IGA* model represents the extended version of the proposed IGA model by equipping the proposed two components on SteganoGAN with different message channels to keep a fair comparison.

3.81% with combined noises on COCO dataset. This shows that our method is able to embed rich information robustly.

Table 2 shows the comparison results of our model with the SteganoGAN model. Note that the SteganoGAN model embeds a message tensor with different channels d instead of a message string. Thus, we equip the proposed two components on SteganoGAN and make corresponding adjustments to our model for multiple-channel message embedding to keep a fair comparison, as the IGA* model shown in the table. From the results, we can see that our method achieves the best performance with different num-

| Methods | COCO | | | | DIV2K | | | |
|-------------|----------|-----------------|--------------|-----------------|--------------|--|--|--|
| | <i>d</i> | <i>Identity</i> | <i>CN</i> | <i>Identity</i> | <i>CN</i> | | | |
| SG | 1 | 27.10 | 30.10 | 39.03 | 43.01 | | | |
| | 2 | 26.43 | 31.87 | 37.56 | 46.02 | | | |
| | 3 | 27.16 | 32.21 | 36.98 | 46.02 | | | |
| | 4 | 27.21 | 31.7 | 38.23 | 46.02 | | | |
| | 5 | 26.88 | 30.8 | 40 | 46.02 | | | |
| IGA* (Ours) | 1 | 31.40 | 32.80 | 43.01 | 43.01 | | | |
| | 2 | 31.10 | 32.04 | 40 | 46.02 | | | |
| | 3 | 30.45 | 32.40 | 46 | 46.02 | | | |
| | 4 | 30.96 | 32.40 | 38 | 46.02 | | | |
| | 5 | 30.83 | 32.59 | 40 | 46.02 | | | |

Table 3. Quantitative comparison of encoded image quality varying different message channels on two datasets, where d denotes the number of message channels. The larger the PSNR values, the better the encoded image. Besides, the first place of each column is bolded and the symbol ‘_’ represents the same performance as the compared model.

ber of message embedding channels under various noises on both datasets. Moreover, it is worth mentioning that our method has better accuracy with message channel $d = 5$ than the SteganoGAN model with message channel $d = 4$ on the COCO dataset and achieves comparable results on the DIV2K dataset. This indicates that our method can embed more information than other models when the accuracy is similar. It also reflects the proposed IGA model plays a positive role to improve model capacity.

4.3. Qualitative Analysis on Imperceptibility and Capacity

Besides the model robustness, the quality of embedded image is also critical for watermarking task. The robustness and imperceptibility is a trade-off. If more messages are in-

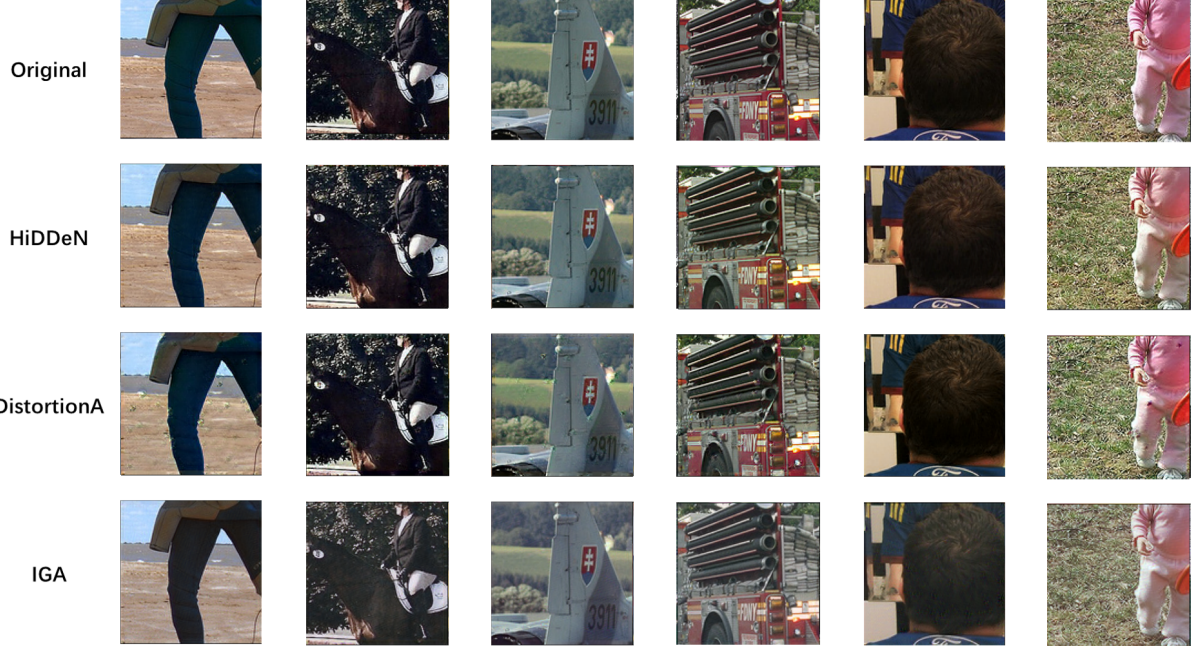


Figure 3. Multiple samples of original and encoded images from the COCO dataset for watermarking task. The first row presents the original cover images. The remaining rows depict the visualization results of the embedded images of the compared models and the proposed IGA model. The “DistortionA” in the figure represents the Distortion-Agnostic model.

tended to be encoded, it will inevitably decline the quality of encoded image. Fig. 3 presents the visualization results of the proposed IGA model and the counterparts, i.e. HiDDeN and Distortion-Agnostic. The figure generally shows our method can not only have exceptional robustness, but also takes the imperceptibility of the embedded image into account. It can be observed that the encoded images generated by our method and the compared methods are visually similar, as well as with cover images. In addition, the PSNR comparison of the proposed IGA model with the SteganoGAN model is provided in Table 3. From the table, our method achieves the best performance in both identity and combined noise settings on the COCO dataset. Moreover, the performance of our method is comparable in most cases on the DIV2K dataset. This experiment proves that our method is more robust under the premise of imperceptibility.

To measure the capacity of watermarking models, Fig. 4 presents the RS-BPP results of our model compared with HiDDeN and Distortion-Agnostic methods. We can observe that the capacity of the model gradually increases with the length increasing of the embedded message. Moreover, the performance of our method is better than the compared methods, whether it is under the case of identity or combined noise settings. In light of this observation, our proposed algorithm is verified to improve the model capacity significantly for more message embedding.

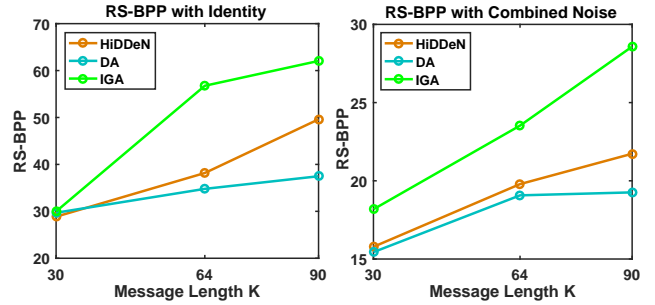


Figure 4. Capacity comparison with HiDDeN and Distortion-Agnostic algorithms on COCO dataset in the case of identity and combined noise settings.

4.4. Ablation Study

In this section, we evaluate the contribution of the message coding module and the inverse gradient attention mask in our proposed method and show the results in Table 4. We conduct experiments on both the COCO and the DIV2K datasets with the message length $K = 90$. From Table 4 we can see that both the message coding module and the inverse gradient attention mask make positive impacts on the performance. And the performance improvement mainly comes from the inverse gradient attention mask.

| Methods | COCO | | DIV2K | |
|---------|--------------|--------------|--------------|--------------|
| | Identity | CN | Identity | CN |
| Basic | 77.56 | 62.07 | 71.04 | 49.84 |
| w MC. | 78.12 | 62.93 | 71.21 | 49.80 |
| w Att. | 84.47 | 65.88 | 71.47 | 55.59 |
| Both | 84.62 | 63.01 | 71.50 | 57.14 |

Table 4. Ablation study results on the COCO and the DIV2K datasets. The first row are the results of the HiDDeN model without our message coding module and inverse gradient attention mask. The following two rows are the results with our message coding module and inverse gradient attention mask respectively. The last row are the results of our full model.

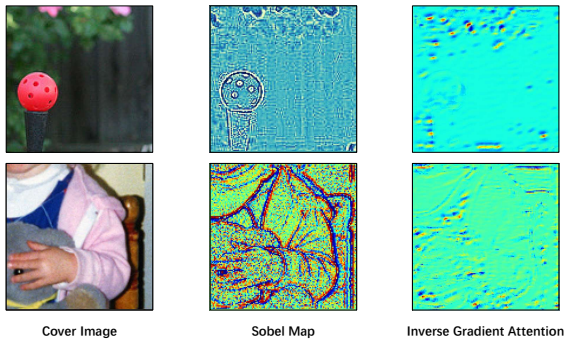


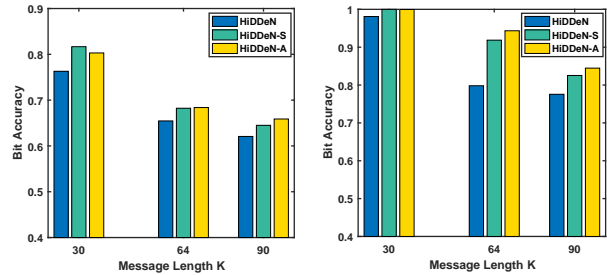
Figure 5. The cover image and its corresponding sobel heatmap and inverse gradient attention heatmap. We perceive that the inverse gradient attention mask is activated strongly in some edge regions similar with the sobel map.

4.5. Discussion

Since our proposed inverse gradient attention map is able to locate pixels which are suitable for message hiding, one can intuitively relate our method to traditional methods which hide messages in texture rich regions. In this section, we compare our IGA mask with edge detection map obtained by the Sobel operator, and discuss the relationship between the proposed IGA mask and the high-frequency map. The experiments show that our IGA map is more suitable for message hiding.

Through the visualization of the inverse gradient attention mask, we perceive that the inverse gradient attention mask is activated strongly in some edge regions, *e.g.*, the map acquired from Sobel operation. So it can be hypothesised that some similarities share by the IGA model with high-frequency areas of an image. Fig. 5 shows the corresponding Sobel Map and Inverse Gradient Attention over cover images. Some similarities between sobel map and inverse gradient attention can be observed.

According to the observation, we further conduct experiments by substituting the inverse gradient attention mask



(a) Results with combined noises. (b) Results without adding noises.

Figure 6. Performance comparison with the inverse gradient attention and the Sobel operator on COCO dataset for watermarking task. The left sub-figure presents the bit prediction accuracy of training and testing with combined noises; the right one shows the performance without adding any noise. Among them, HiDDeN-S represents the algorithm using Sobel edge operator, and HiDDeN-A represents our algorithm with inverse gradient attention mask to perform digital watermarking task.

with the Sobel map for our digital watermarking framework. The comparative experimental results are shown in the Fig. 6. It can be seen that by adopting the Sobel map for digital watermarking, the model also achieves promising performance. The experimental result empirically shows attending pixels with rapidly changing frequency (*i.e.*, edge regions) generally has a similar effect as inverse gradient attention for model robustness enhancement. It is further discovered that the proposed IGA model receives better results on all cases than the model with Sobel map, due to the proposed IGA mechanism is able to attend pixels adaptively toward robust message hiding. It also indicates that not all edge regions are suitable for information hiding.

5. Conclusion

In the paper, we propose a novel end-to-end deep watermarking model with Inverse Gradient Attention (IGA) mechanism, which allows the model to mine more robust pixels for data hiding. The model equipped with the proposed IGA mask is able to adaptively and robustly embed more desired data. Besides, we adopt a symmetric message coding module, as known as Message Encoder and Decoder in our framework, to constrain the message recovery in a reduced dimension. It further improves the capacity of embedding information. Moreover, we further identify and discuss the connections between the proposed inverse gradient attention with high-frequency regions within images. From extensive experimental results, our proposed IGA model is able to achieve superior performance than current state-of-the-art methods.

References

- [1] E. Agustsson and R. Timofte. Ntire 2017 challenge on single image super-resolution: Dataset and study. In *IEEE Conf. Comput. Vis. Pattern Recog. Worksh.*, pages 1122–1131, 2017. 5
- [2] Shumeet Baluja. Hiding images in plain sight: Deep steganography. In *Adv. Neural Inform. Process. Syst.*, pages 2069–2079, 2017. 2
- [3] A. Bamatraf, R. Ibrahim, and M. N. B. M. Salleh. Digital watermarking algorithm using lsb. In *Int. Conf. Comp. App. Ind. Ele.*, pages 155–159, 2010. 2
- [4] Amin Banitalebi, Said Nader-Esfahani, and Alireza Nasiri Avanaki. Robust LSB watermarking optimized for local structural similarity. *arXiv preprint arXiv:1803.04617*, 2018. 2
- [5] W. Bender, D. Gruhl, N. Morimoto, and A. Lu. Techniques for data hiding. *IBM Sys. Jour.*, 35(3.4):313–336, 1996. 1
- [6] Ning Bi, Qiyu Sun, Daren Huang, Zhihua Yang, and Jiwu Huang. Robust image watermarking based on multiband wavelets and empirical mode decomposition. *IEEE Trans. Image Process.*, 16(8):1956–1966, 2007. 2
- [7] Ian J. Goodfellow, Jonathon Shlens, and Christian Szegedy. Explaining and harnessing adversarial examples. In *Int. Conf. Learn. Represent.*, 2015. 1, 3
- [8] Diederik P. Kingma and Jimmy Ba. Adam: A method for stochastic optimization. In *Int. Conf. Learn. Represent.*, 2015. 5
- [9] D. Kundur and D. Hatzinakos. Digital watermarking using multiresolution wavelet decomposition. In *ICASSP*, volume 5, pages 2969–2972, 1998. 1
- [10] Tsung-Yi Lin, Michael Maire, Serge J. Belongie, James Hays, Pietro Perona, Deva Ramanan, Piotr Dollár, and C. Lawrence Zitnick. Microsoft COCO: common objects in context. In *Eur. Conf. Comput. Vis.*, volume 8693, pages 740–755, 2014. 5
- [11] Jianfeng Lu, Meng Wang, Junping Dai, Qianru Huang, Li Li, and Chin-Chen Chang. Multiple watermark scheme based on DWT-DCT quantization for medical images. *J. Inf. Hiding Multim. Signal Process.*, 6(3):458–472, 2015. 2
- [12] Xiyang Luo, Ruohan Zhan, Huiwen Chang, Feng Yang, and Peyman Milanfar. Distortion agnostic deep watermarking. In *IEEE Conf. Comput. Vis. Pattern Recog.*, pages 13545–13554, 2020. 1, 2, 3, 4, 5
- [13] Seung-Min Mun, Seung-Hun Nam, Han-Ul Jang, Dongkyu Kim, and Heung-Kyu Lee. A robust blind watermarking using convolutional neural network. *arXiv preprint arXiv:1704.03248*, 2017. 2
- [14] Shabir A. Parah, Javaid A. Sheikh, Nazir A. Loan, and Ghulam Mohiuddin Bhat. Robust and blind watermarking technique in DCT domain using inter-block coefficient differencing. *Digit. Signal Process.*, 53:11–24, 2016. 2
- [15] Tomás Pevný, Tomás Filler, and Patrick Bas. Using high-dimensional image models to perform highly undetectable steganography. In *Int. Conf. Inf. Hid.*, volume 6387, pages 161–177, 2010. 2
- [16] Farzin Yaghmaee and Mansour Jamzad. Estimating watermarking capacity in gray scale images based on image complexity. *EURASIP J. Adv. Signal Process.*, 2010, 2010. 3
- [17] Chong Yu. Attention based data hiding with generative adversarial networks. In *AAAI*, pages 1120–1128, 2020. 1, 2
- [18] Kevin Alex Zhang, Alfredo Cuesta-Infante, Lei Xu, and Kalyan Veeramachaneni. Steganogan: High capacity image steganography with gans. *arXiv preprint arXiv:2001.09678*, 2019. 5
- [19] Jiren Zhu, Russell Kaplan, Justin Johnson, and Li Fei-Fei. Hidden: Hiding data with deep networks. In *Eur. Conf. Comput. Vis.*, 2018. 1, 2, 5